HHS Public Access

Author manuscript

FASEB J. Author manuscript; available in PMC 2023 May 29.

Published in final edited form as:

FASEB J. 2023 February ; 37(2): e22761. doi:10.1096/fj.202200994R.

STAT6 suppression prevents bleomycin-induced dermal fibrosis

Jingjing Huang[1,2], **Hydia Puente**[2,3], **Nancy E. Wareing**[2,3], **Minghua Wu**[3], **Maureen D. Mayes**[3], **Harry Karmouty-Quintana**[2], **Shervin Assassi**[3], **Tingting W. Mills**[2]

[1]Department of Geriatrics, The Fourth Affiliated Hospital of Nanjing Medical University, Nanjing, Jiangsu, China

[2]Department of Biochemistry and Molecular Biology, McGovern Medical School, The University of Texas Health Science Center at Houston, Houston, Texas, USA

[3]Department of Internal Medicine, Division of Rheumatology, The University of Texas Health Science Center at Houston, Houston, Texas, USA

Abstract

Fibrosis of the skin and internal organs is a hallmark of systemic sclerosis (SSc). Although the pathogenesis of SSc is poorly understood, increasing evidence suggests that interleukins (IL)-4 and − 13 contribute to the pathogenesis of skin fibrosis by promoting collagen production and myofibroblast differentiation. Signal transducers and activators of transcription 6 (STAT6) is one of the most important downstream transcription factors activated by both IL-4 and IL-13. However, it is not completely understood whether STAT6 plays a role during the pathogenesis of skin fibrosis in SSc. In this study, we observed increased STAT6 phosphorylation in fibrotic skin samples collected from SSc patients as well as bleomycin-injected murine mice. Knockout of Stat6 in mice significantly (1) suppressed the expression of fibrotic cytokines including *Il13, Il17, Il22, Ccl2*, and the alternatively activated macrophage marker *Cd206*; (2) reduced the production of collagen and fibronectin, and (3) attenuated late-stage skin fibrosis and inflammation induced by bleomycin. Consistently, mice treated with STAT6 inhibitor AS1517499 also attenuated skin fibrosis on day 28. In addition, a co-culture experiment demonstrated that skin epithelial cells with STAT6 knockdown had reduced cytokine expression in response to IL-4/IL-13, and subsequently attenuated fibrotic protein expression in skin fibroblasts. On the other side, STAT6 depletion in skin fibroblasts attenuated IL-4/IL-13-induced cytokine and fibrotic marker expression, and reduced *CXCL2* expression in co-cultured keratinocytes. In summary, our study highlighted an important yet not fully understood role of STAT6 in skin fibrosis by driving innate inflammation and differentiation of alternatively activated macrophages in response to injury.

Correspondence Tingting W. Mills, Department of Biochemistry and Molecular Biology, McGovern Medical School at UTHealth, Houston, TX 77030, USA. tingting.weng@uth.tmc.edu.

AUTHOR CONTRIBUTIONS

Tingting W. Mills, Minghua Wu, and Shervin Assassi designed the experiments. Jingjing Huang, Hydia Puente, and Tingting W. Mills performed the experiments. Jingjing Huang, Nancy E. Wareing, and Tingting W. Mills analyzed the data. Tingting W. Mills and Jingjing Huang drafted the manuscripts. Nancy E. Wareing, Minghua Wu, Shervin Assassi, Harry Karmouty-Quintana revised and edited the manuscript. Maureen D. Mayes, Tingting W. Mills, Harry Karmouty-Quintana, and Shervin Assassi provided resources.

DISCLOSURES

The authors have stated explicitly that there are no conflicts of interest in connection with this article.

SUPPORTING INFORMATION

Additional supporting information can be found online in the Supporting Information section at the end of this article.

Keywords

cytokine; IL-13; IL-4; skin fibrosis; STAT6; systemic sclerosis

1 | INTRODUCTION

Systemic sclerosis (SSc) is a rare autoimmune disease characterized by fibrosis of multiple organs, autoimmunity, as well as vascular damage.[1] Skin tightening and fibrosis is one of the major features of SSc that are normally associated with the overproduction of extracellular matrix (ECM) proteins, including collagen type I, type III, fibronectin, and aminoglycans by myofibroblasts in the connective tissues.[2] Although the mechanisms that lead to fibrosis of the skin and visceral organs in SSc have been studied to some extent, the development of effective therapeutic agents for SSc fibrotic complications is hampered due to an incomplete understanding of the disease pathophysiology.

Several profibrogenic cytokines have been reported to modulate the proliferation and deposition of ECM proteins by fibroblasts. Transforming growth factor-β (TGFβ) is the key cytokine of tissue fibrosis that promotes the synthesis of collagens and fibronectins.[3] Th2 cytokines including interleukin-4 and -13 (IL-4 and IL-13) have been shown to have increased levels in the serum of SSc patients compared to controls.[4] Both cytokines have been reported to promote the transcription of collagen genes in dermal fibroblasts.[5,6] Several studies indicated that IL-4 and IL-13 facilitate TGFβ-induced fibrosis by promoting the expression of TGFβ,[7–9] suggesting complex interactions and co-regulation among multiple cytokines during the pathogenesis of fibrosis.

Interestingly, IL-4 and IL-13 share common receptor complexes and can both signal through Janus kinase 1 (JAK1) and signal transducers and activators of transcription 6 (STAT6).[10] The activation of their receptors induces JAK1 tyrosine phosphorylation. Phosphorylated JAK1 permits tyrosine phosphorylation of STAT6 on residue Y641.[11,12] The phosphorylated STAT6 forms homo- or hetero-dimers which translocate into the nucleus and bind to the STAT-responsive element (SRE), facilitating the expression of target genes.[13] IL-4 and IL-13 have over-lapping functions as they share a common receptor and both signal through the STAT6 pathway.[14] The role of IL-4 and IL-13 in fibrosis and fibroblast activity has been emphasized in several studies. Both IL-4 and IL-13 have been reported to induce myofibroblast differentiation from fibroblasts and promote the expression and deposition of ECMs in vitro.[15,16] Moreover, IL-4 overexpression under the control of an insulin promoter stimulated pancreatic fibrosis,[17] while blocking IL-4 signaling with anti-IL-4 antibodies prevented skin fibrosis in tight skin (TSK1) mice.[18] Similarly, neutralization of IL-13 attenuated bleomycin-induced lung fibrosis in mice.[19,20] Consistent with these findings, Romilkimab, an antibody neutralizing IL-4/-13 is currently in a clinical trial for the treatment of early diffuse cutaneous SSc.[21] Because STAT6 is the most critical downstream transcription factor of IL-4 and IL-13, these findings suggest a potential role of STAT6 signaling in skin fibrosis in SSc. Indeed, STAT6 was found hyper-activated in hypochlorous acid-induced skin and lung fibrosis, and Leflunomide (a drug to treat rheumatoid arthritis) attenuated skin and lung fibrosis is associated with STAT6 inhibition.[22]

Moreover, a previous study using a JAK-STAT6 inhibitor suggested that inhibition of the STAT6 signal prevents Th2 cytokine-stimulated eotaxin-3 expression in both fibroblasts and epithelial cells,[23] supporting JAK-STAT6 inhibition as a novel approach to treating inflammation and fibrosis. However, it remains elusive whether STAT6 is activated in SSc skin, and whether a specific STAT6 inhibition could attenuate skin fibrosis. Moreover, few studies were reported using genetically modified mice to understand the role of STAT6 in skin fibrosis.

The goal of the present study was to examine the role of STAT6 in skin fibrosis. We observed significantly increased STAT6 phosphorylation in epidermal and dermal cells of fibrotic skin collected from SSc patients and bleomycin-treated mice. Next, using the repetitive bleomycin-induced murine skin fibrosis model, we found that mice with Stat6 knockout or treated with STAT6 inhibitor AS1517499 attenuated late-stage skin fibrosis. Moreover, in vitro co-culture demonstrated an important role of STAT6 in epithelial and fibroblast crosstalk by regulating cytokines release. Taken together, our data demonstrated that STAT6 activation could promote skin fibrosis by dysregulating the normal epithelial-fibroblasts interactions.

2 | MATERIALS AND METHODS

2.1 | Human samples

Skin biopsy samples were collected from SSc patients and age-, gender-, and ethnicity-matched healthy controls from the Genetic versus Environment In Scleroderma Outcome Study (GENISOS) cohort at UTHSC at Houston (See Table S1 for the patient and control information). All patients included had affected skin at the site of the biopsy. The healthy control subjects had no personal or family medical history of autoimmune diseases. All subjects provided written informed consent, and the study was approved by the institutional review boards at UTHSC.

2.2 | Cell culture and treatment

The skin keratinocyte cell line HaCaT was purchased from AddexBio and cultured in modified Dulbecco's Modified Eagle Medium (DMEM) (AddexBio) containing 10% fetal bovine serum (FBS) and 1% antibiotics to avoid contamination. Primary human skin fibroblasts were isolated using an out-growth model from skin biopsies from normal donors and SSc patients. Isolated fibroblasts were cultured in DMEM (Sigma-Aldrich) containing 10% FBS (FBS) and 1% antibiotics, and mycoplasma infection was tested using the MycoAlert™ Mycoplasma Detection Kit (Lonza). Passage 4–6 fibroblasts were used. Cell culture was maintained at 37°C in a humidified 5% carbon dioxide atmosphere.

For the co-culture experiment, *STAT6* was knocked down in skin keratinocyte HaCaT cells (or primary human skin fibroblasts) with non-targeting (negative control) or *STAT6* siRNA (50 picomole/ml, Sigma-Aldrich) and lipo-fectamine RNAimax (Thermo Fisher Scientific). Two days after transfection, cells were stimulated with both IL-4 and IL-13 (10 ng/ml each) for 6 h. The cell media were then changed to IL-4/IL-13 free media, and the keratinocytes (or human skin fibroblasts) were co-cultured with primary skin fibroblasts (or HaCaT) that

were plated in cell culture inserts for an additional 24 h before harvesting RNA and protein for analysis.

2.3 | Masson's trichrome stain and immunohistochemistry (IHC)

Human or mouse skin were fixed in 10% phosphate-buffered formalin for at least 24 h, dehydrated, paraffin-embedded, and sectioned at a thickness of 4 μm. For Masson's trichrome staining, skin sections were deparaffinized, rehydrated, and stained using the trichrome stain (Masson) Kit (Sigma-Aldrich). Images were taken from an Olympus BX60 equipped with a DP71 camera. The dermal thickness of Masson's trichrome-stained skin was blindly measured by a well-trained technician using ImageJ (National Institutes of Health). Three randomly selected areas were measured per skin and data were presented as mean ± standard error.

For IHC, sections were dewaxed in Histo-Clear (National Diagnostics) and rehydrated in a series of ethanol solutions. Then, the sections were quenched with 3% hydrogen peroxide and incubated in 1X citrate buffer (VectorLabs) for antigen retrieval. After that, sections were incubated with BLOXALL® Endogenous Blocking Solution (VectorLabs) followed by blocking with 5% normal goat serum. Then sections were incubated with primary antibodies overnight at 4°C. The following primary antibodies were used for this study: p-STAT6 (1:200, rabbit polyclonal, Abcam), Mac-3 (1: 50, rabbit polyclonal, BD Biosciences), and CD3 (1:800, rabbit polyclonal, Proteintech). After primary antibody incubation, slides were then incubated with ImmPRESS anti-rabbit secondary antibodies (VectorLabs) for 1 h at room temperature. After rinsing, human slides were developed with Vector Red (VectorLabs) and counter-stained with 4′,6-diamidino-2-phenylindole (DAPI) (VectorLabs). And mouse slides were developed with DAB Substrate Kit (VectorLabs) and counter-stained with Vector hematoxylin (VectorLabs).

2.4 | Animals and treatment

The wildtype C57BL/6 and *Stat6* knockout (*Stat6*$^{-/-}$, strain # 005977) mice were purchased from the Jackson Laboratory. Mice were maintained under specific pathogen-free conditions in our animal facility. The use of animals was in full compliance with the Animal Welfare Committee. No evidence of fungal, parasitic, or bacterial infection was observed.

The mouse model of skin fibrosis was generated by repetitive subcutaneous (s.q.) bleomycin (Teva Pharmaceuticals, Northwales, PA) injection. Briefly, 8-week-old female C57BL/6 or *Stat6*$^{-/-}$ mice were anesthetized with isoflurane using an isoflurane vaporizer. Bleomycin in phosphate-buffered saline (0.02 U/mouse/day) was injected subcutaneously into two locations on the shaved dorsum of the mice six times per week for 2 or 4 weeks. For mice treated with STAT6 inhibitor AS1517499, 100 ul AS1517499 (0.1 mg/ml in 20% Dimethyl sulfoxide (DMSO)) were subcutaneously injected twice a week starting 1 week after the initial bleomycin injection at the same locations. Mice injected with 20% DMSO were used as controls. The mouse skin was collected for real-time qRT-PCR, histology, and western blot analysis on day 14 or day 28 after the first bleomycin injection.

2.5 | Real-time quantitative reverse transcription PCR (real-time qRT-PCR)

Skin tissues were homogenized using TRIZOL Reagent (Thermo Fisher Scientific, MA), and total RNA was extracted using RNeasy Mini Kit (Qiagen, MD). Extracted RNA was treated with Heat & Run gDNA remover kit (ArcticZymes, PA) to remove the genomic DNA, and reverse transcribed into cDNA using iScript™ cDNA Synthesis Kit (Bio-Rad, CA). Real-time qRT-PCR was carried out with Roche LightCycler 96 using the primers defined in Table S2. The data were quantified using the comparative Ct method and presented as mean ratio to β-actin ± standard error.

2.6 | Western blot

Skin samples were homogenized in RIPA lysis buffer (50 mM Tris–HCl pH 7.4, 150 mM NaCl, 1% NP-40) containing both protease and phosphatase inhibitor cocktail (Thermo Fisher Scientific, NJ). The same amount of protein was loaded on the sodium dodecyl sulfate-polyacrylamide gels for electrophoresis. Protein was then transferred from the gels to polyvinylidene fluoride membrane sheets. After blocking with 5% milk in TBST (Tris-buffered saline, 0.1% Tween 20) buffer for 1 h, the membranes were incubated with primary rabbit anti-collagen 1 (Abcam, AB21286), rabbit anti-fibronectin (Sigma-Aldrich, F3648), mouse anti-β-actin (Sigma-Aldrich, A3854), or mouse anti-α-SMA antibodies (Sigma-Aldrich, ABT1487) at 4°C overnight, and then incubated with corresponding secondary antibodies conjugated to horseradish peroxidase (Cell Signaling Technology). Finally, the membranes were developed with Pierce ECL Western Blotting Substrate (Thermo Fisher Scientific) and visualized with a Bio-Rad Gel Doc imaging system.

2.7 | Statistical analysis

All statistical analysis were carried out using GraphPad Prism 6.0 (San Diego). Data were presented as mean ± standard error. Two-tailed unpaired Student's *t*-test was used to compare the statistical significance between two treatment groups. A p-value <.05 was considered to be statistically significant.

3 | RESULTS

3.1 | STAT6 is activated in the fibrotic skin of SSc patients

To understand the role of STAT6 in skin fibrosis, we first carried out immunohistochemistry (IHC) to determine whether fibrotic skin had increased STAT6 activation. As shown in Figure 1A, SSc skin had increased phosphorylated-STAT6 (p-STAT6)-positive cells in both the epidermal and dermal layers compared to normal controls. Blinded cell counting indicated that the number of p-STAT6-positive cells at both epidermal and dermal layers per field was significantly elevated in SSc skin tissues compared to normal controls (Figure 1B). Consistent with these findings, p-STAT6 protein levels were elevated in 4 out of 5 primary skin fibroblasts isolated from SSc patients compared to those from normal donors (Figure 1C). To understand whether p-STAT6 elevation could also be observed in a murine model of fibrosis, we used a repetitive bleomycin-induced skin fibrosis model to induce skin fibrosis in mice. In this model, bleomycin was subcutaneously injected six times a week for 2 or 4 weeks. This model is an inflammation-driven skin fibrosis model that is initiated

with a massive inflammation response that peaks within the first 2 weeks, and progressed with increased ECM deposition and significant dermal fibrosis observed at the 4-week time point.[24,25] Similarly, p-STAT6 staining was also observed in day 28 bleomycin-injected murine skin in both epidermal, especially at the sites of injections (Figure 1D, middle panel), and dermal layers (Figure 1C, right panel). Quantification analysis suggested increased p-STAT6 cells at both epidermal and dermal layers in bleomycin skin compared to PBS skin (Figure 1E). In summary, these results indicate that STAT6 is activated in both human and mouse fibrotic skin, and abrogated expression or activation of STAT6 may contribute to the pathogenesis of fibrosis in SSc patients.

3.2 | STAT6 depletion increases fibrotic marker expression but not dermal thickness in the early stage of bleomycin-induced injury

Given the critical role of IL-4 and IL-13 in dermal fibrosis, we hypothesize that their downstream transcription factor STAT6 also contributes to skin fibrosis. Here, we used the repetitive bleomycin-induced skin fibrosis model to induce skin fibrosis in both wild type (WT) and *Stat6* knockout (*Stat6*$^{-/-}$) mice. The Stat6$^{-/-}$ mice are viable and fertile, and do not show any behavioral abnormalities compared to the WT mice.[26] Because SSc is more prevalent in female patients (female to male ratio of 3:1),[27] only female mice were selected for our following experiments. As shown in Figure 2A, the *Stat6* transcript levels were significantly suppressed in the *Stat6*$^{-/-}$ mice, suggesting a successful *Stat6* deletion. After exposure to 14 days of bleomycin, at which point inflammation accommodates the initiation of fibrosis, *Stat6*$^{-/-}$ mice had decreased protein levels of type I collagen (COL1) and fibronectin (FN1) compared to WT controls (Figure 2B). However, Masson's trichrome staining showed that the collagen deposition and dermal thickness did not differ significantly between *Stat6*$^{-/-}$ and WT mice (Figure 2C,D). To understand whether there is any difference in the inflammation, we performed IHC using Mac-3 (maker for macrophages, lysosome-associated membrane protein 2, also known as LAMP2) and CD3 (marker for T cells) antibodies. There are a lot of Mac-3-positive cells but very few CD3-positive cells in both *Stat6*$^{-/-}$ and WT mice. This is consistent with Dr. Varga's findings that macrophages are more abundant inflammatory cells than T cells in bleomycin-induced skin fibrosis in mice.[28] No difference was observed in the number of either Mac-3-positive (Figure 2D) or CD3-positive (data not shown) cells in *Stat6*$^{-/-}$ mice compared to WT controls. Moreover, the transcript levels of fibrotic markers collagen 1 alpha 1 (*Col1a1*), fibronectin (*Fn1*), and periostin (*Postn*) are not significantly changed in *Stat6*$^{-/-}$ mice (Figure 2E).

In addition to directly inducing ECM expression in fibroblasts,[29] the type 2 cytokines IL-4 and IL-13 through STAT6 activation can also promote alternative macrophage activation and may subsequently contribute to skin fibrosis.[30,31] To understand the role of STAT6 in skin inflammation, the transcript expression of several cytokines including *Il4* and *Il13* was determined. *Il4* but not *Il13* had a trend of elevated expression in bleomycin-treated *Stat6*$^{-/-}$ skin (Figure 2F). Consistent with the anti-inflammatory role of *Il4* and *Il13* through *Stat6* activation,[32] knockout of *Stat6* increased the expression of pro-inflammatory cytokines including the chemokine (C-X-C motif) ligand 1 and 2 (*Cxcl1* and *Cxcl2*) and *Il6* in *Stat6*$^{-/-}$ skin (Figure 2F). Taken together, these results show the absence of *Stat6* may promote inflammatory cytokine release without affecting macrophage infiltration, and suppresses

bleomycin-induced ECM protein production at the early stage, but these changes are not sufficient to decrease dermal thickness.

3.3 | Stat6 depletion attenuates bleomycin-induced skin fibrosis on day 28

To understand the chronic effects of *Stat6* depletion on skin fibrosis, lesional skin samples were also collected for analysis on day 28 after the initial bleomycin injection, a stage when there is fulminant skin fibrosis. The protein expression of the fibrotic markers collagen 1 and fibronectin was markedly decreased in the skin of *Stat6*$^{-/-}$ mice treated with bleomycin compared to WT controls (Figure 3A). Masson's trichrome staining indicated that the collagen deposition was reduced in the dermal layer and the dermal thickness was significantly decreased in *Stat6*$^{-/-}$ mice (Figure 3B,C). Mac-3 IHC showed reduced macrophage infiltration in *Stat6*$^{-/-}$ mice compared to WT controls (Figure 3C). Consistent with these findings, real-time qRT-PCR analysis of fibrotic markers showed significantly suppressed *Col1a1, Fn1*, and *Postn* in day 28 *Stat6*$^{-/-}$ skin tissues compared to WT controls (Figure 3D), suggesting reduced end-stage skin fibrosis in *Stat6*$^{-/-}$ mice. Interestingly, *Il13* had significantly decreased expression on day 28 bleomycin-treated *Stat6*$^{-/-}$ skin compared to WT controls (Figure 3E), suggesting that its downregulation may account for the decreased fibrosis in *Stat6*$^{-/-}$ skin. Moreover, cytokines including *Cxcl10*, *Il17*, *Il22*, and C-C Motif Chemokine Ligand 2 (*Ccl2*) were dramatically decreased in *Stat6*$^{-/-}$ skin (Figure 3E). In line with the known roles of IL-4/IL-13/STAT6 in alternative macrophage polarization,[33] the level of alternatively activated macrophage (M2) marker *Cd206* was significantly decreased in day 28 *Stat6*$^{-/-}$ skin (Figure 3E).

However, the pro-inflammatory cytokines that were induced on day 14 were no longer elevated in day 28 *Stat6*$^{-/-}$ skin (Figure 3E). Overall, our data indicated that bleomycin-induced skin fibrosis and macrophage infiltration were significantly attenuated in *Stat6*-depleted mice at the fibrotic stage possibly by suppressing the release of cytokines and inhibiting the infiltration and differentiation of alternatively activated M2 macrophages.

3.4 | STAT6 inhibitor AS1517499 alleviates bleomycin-induced skin fibrosis

Next, we are interested to see whether skin fibrosis could be ameliorated through pharmacologically inhibiting STAT6. AS1517499 is an effective STAT6 inhibitor that has been shown to prevent renal fibrosis by attenuating fibroblast activation and macrophage polarization in mice.[34] However, the role of AS1517499 has not been demonstrated in skin fibrosis. As shown in Figure 4, mice treated with AS1517499 had significantly decreased p-STAT6, collagen and fibronectin protein expression (Figure 4A), reduced skin thickness (Figure 4B), and collagen deposition (Figure 4C), number of Mac-3-positive cells (Figure 4C) and declined transcript expression of *Col1a1 and Fn1* (Figure 4D). Consistently with the findings in the *Stat6*$^{-/-}$ skin, AS1517499-treated skin had decreased *Il13* transcript levels, as well as the levels of M2 macrophage marker *Cd206* (Figure 4E). Although some of the fibrotic cytokines reduced in *Stat6*$^{-/-}$ skin is not changed in AS1517499-treated lesional skin, the transcript level of *Tgfb1* was significantly downregulated (Figure 4E), suggesting that inhibiting *Tgfb1* may partially contribute to the role of STAT6 in skin fibrosis. Taken together, these data suggest that pharmacological STAT6 inhibition by AS1517499 could attenuate skin fibrosis induced by bleomycin.

3.5 | STAT6 depletion prevents cytokine expression in keratinocytes and attenuates the fibrotic marker induction in co-cultured skin fibroblasts

We next performed in vitro studies to determine whether STAT6 activation in dermal keratinocytes has a direct impact on fibrotic marker expression in fibroblasts. Immortalized epidermal keratinocytes (HaCaT) were transfected with STAT6-targeting siRNA to knock down STAT6 (Figure 5A). Transfected HaCaT cells were then stimulated with IL-4/IL-13 together and co-cultured with primary skin fibroblasts. As shown in Figure 5B, STAT6 depletion significantly repressed the IL-4/IL-13-induced transcript expression of cytokines including, *CCL2, CXCL2, IL6, IL17, and TGFB1*. Interestingly, the protein levels of POSTN and COL1, as well as the transcript levels of *POSTN*, *COL1A1*, and *FN1* were all decreased in fibroblasts co-cultured with keratinocytes transfected with *STAT6* siRNA compared to those transfected with non-targeting-control-siRNA (Figure 5C,D). Although the protein levels of COL1 were not increased by IL-4/IL-13 stimulation, they were suppressed at the baseline levels in fibroblasts cultured with STAT6 siRNA transfected keratinocytes, a finding possibly attributable to post-transcriptional mechanisms or other cytokines. Altogether, our data suggest that STAT6 depletion in keratinocytes attenuates fibrotic marker induction in co-cultured skin fibroblasts possibly by repressing cytokine release from keratinocytes.

3.6 | Fibroblasts STAT6 activation promotes *CXCL2* expression in co-cultured keratinocytes

Given the roles of epithelial STAT6 activation on fibroblast differentiation, it is interesting to know whether fibroblast STAT6 activation affects keratinocytes activation and differentiation. To address this question, primary human skin fibroblasts were transfected with control or STAT6-targeting siRNA to knock down STAT6 (Figure 6A). Transfected HaCaT cells were then stimulated with IL-4/IL-13. As shown in Figure 6A, IL-4/and Il-13 activated STAT6 phosphorylation 2 h after stimulation and led to increased COL1 and POSTN protein expression after 24 h. STAT6 silence significantly repressed the COL1 and POSTN induction. Moreover, STAT6 knockdown suppressed IL-4/IL-13-induced transcript expression of cytokines including *CCL2, CXCL2*, and *IL6* (Figure 6B). Although *IL8* and *IL17* levels were not induced by IL-4/IL-13, they were downregulated in fibroblasts with STAT6 knockdown (Figure 6B). And as what others reported, STAT6 repression attenuated IL-4/IL-13 mediated POSTN induction (Figure 6C).[35] Interestingly, the transcript levels of *CXCL2* were highly induced in keratinocytes co-cultured with fibroblasts treated with IL-4/Il-13 and this induction is absent in keratinocytes co-cultured with fibroblasts transfected with *STAT6* siRNA (Figure 6D). The transcript levels of *CCL2, CXCL1, Il1B*, and *IL* 6 were not affected. No protein or transcript expression of fibrotic markers COL1, FN1, and POSTN were detected in keratinocytes (data not shown), suggesting that STAT6 activation in fibroblasts is not sufficient to induce epithelial-to-mesenchymal differentiation of co-cultured keratinocyte. Overall, our data suggest that STAT6 activation in fibroblasts induces CXCL2 release from keratinocytes.

4 | DISCUSSION

SSc is a rare life-threatening autoimmune disease that has massive fibrosis in the skin and several visceral organs. The role of IL-4 and IL-13 in myofibroblast differentiation and ECM production has been reported in several independent studies.[16] STAT6 is the most critical downstream transcription factor that can be activated by both IL-4 and IL-13. However, few studies were carried out to understand the role of STAT6 in skin fibrosis in SSc. Here, we demonstrate for the first time that STAT6 phosphorylation is elevated in fibrotic skin from SSc patients or bleomycin-treated mice. STAT6 knockdown in keratinocytes attenuates the fibrotic marker induction in co-cultured skin fibroblasts possibly by repressing the cytokine release from keratinocytes. While STAT6 inhibition in fibroblasts reduced CXCL2 release from keratinocytes. Moreover, *Stat6* depletion or inhibition attenuated the development of bleomycin-induced skin fibrosis in mice by regulating the expression of fibrotic cytokines.

IL-4 and IL-13 are the major cytokines that activate STAT6. Both (IL-4 and IL-13) have been shown to have increased levels in the serum of SSc patients compared to controls,[4] and their inhibition is associated with attenuated skin and lung fibrosis in mice.[18–20] These findings suggested that STAT6, the most critical downstream transcription factor of IL-4 and IL-13, may also play a role in skin fibrosis in SSc. Consistently, several lines of studies indicate that STAT6 is implicated in tissue fibrosis including lung, kidney, and skin fibrosis.[36–39] In bleomycin-induced pulmonary fibrosis in mice, STAT6 phosphorylation was elevated along with enhanced IL-4 and IL-13 levels. In addition, in bleomycin-injected Sphingosine-1-phosphate receptor-2 (Sipr2) knockout mice that had alleviated pulmonary fibrosis compared to WT controls, STAT6 phosphorylation was diminished, suggesting that STAT6 may mediate S1PR2 facilitates lung fibrosis.[36] Moreover, *Stat6*$^{-/-}$ mice showed suppressed acute inflammation and pulmonary fibrosis in response to multi-walled carbon nanotube administration.[37] Consistent with the finding in lung fibrosis, STAT6 was activated in renal fibrosis, and *Stat6*-deficient mice had decreased accumulation of bone marrow-derived fibroblasts, reduced ECMs production, and attenuated fibrosis in obstructed kidney.[38] More relevant to our study, Stat6 depletion in tight-skin mice had been shown to suppress skin fibrosis.[39] Similar to these findings, we determined for the first time that the STAT6 phosphorylation was increased in the fibrotic skin of SSc patients. Moreover, using genetically modified mice and a repetitive bleomycin-induced skin fibrosis model, we observed a decreased ECM production, and attenuated skin fibrosis in *Stat6*$^{-/-}$ mice, suggesting that STAT6 plays a critical role in skin fibrosis in SSc. Consistently, mice treated with STAT6 inhibitor AS1517499 attenuated skin fibrosis on day 28, indicating that targeting STAT6 with AS1517499 could be a novel therapeutic approach for skin fibrosis.

Bleomycin-induced skin fibrosis has substantial inflammation, especially at the early stages of injury.[24,25] Consistent with previous findings showing the anti-inflammatory role of Th2 cytokine IL-4 and IL-13, as well as the studies in various models including EAE and diabetes showing that *Stat6*$^{-/-}$ mice have increased inflammation,[40,41] our findings demonstrated that *Stat6* depletion promoted the production of skin pro-inflammatory cytokines on day 14 after initial bleomycin injection, including *Cxcl1* and *Cxcl2*. Although it was not statistically significant, there was a trend of increased expression of *Il4, Il17*, and *Il22* in the skin of *Stat6*$^{-/-}$ mice injected with bleomycin, indicating that the overall

inflammation was increased in the *Stat6*$^{-/-}$ mice in response to bleomycin at the early stage. Interestingly, at the late fibrotic stage (day 28 after initial bleomycin injection), no difference was detected in the expression of *Il4, Cxcl1*, and *Cxcl2*, while the expression of *Cxcl10*, *Il17*, and *Il22* was significantly suppressed in *Stat6*$^{-/-}$ mice. *Cxcl10* levels are significantly elevated in the serum and tissue of SSc patients.[42,43] Both IL17 and IL22 are type 3 cytokines and they have been recognized to play profibrogenic roles in various tissue fibrosis including TGFβ-dependent liver fibrosis,[44] intestine fibrosis,[45] cystic fibrosis,[46] and skin fibrosis.[47] Consistent with the findings in animal models, the co-culture experiment also demonstrated a reduction of *IL17* and *IL22* in keratinocytes with STAT6 knockdown. TGFβ, the key pro-fibrotic growth factor also shows a trend of reduction in STAT6-depleted keratinocytes. And the reduction of these cytokines is associated with suppressed fibrotic marker expression in co-cultured skin fibroblasts. *Il17* is also suppressed in fibroblasts with STAT6 depletion, suggesting that fibroblasts could be an additional source of IL17 in SSc. Taken together, these findings suggested that STAT6-regulated *Il17* and *Il22* may be associated with the decreased expression of ECMs proteins and RNAs, as well as attenuated skin fibrosis in *Stat6*$^{-/-}$ mice treated with bleomycin.

Macrophages/monocytes are normally classified into two phenotypes: classically activated (M1) phenotype that is pro-inflammatory, and alternatively activated (M2) phenotype that is often profibrotic and anti-inflammatory.[30,31] One of the important roles of IL-13 and IL-4 is to promote the alternative M2 macrophage activation, and over-activation of M2 macrophages has been shown to contribute to fibrosis.[30] The critical function of M2 macrophage in promoting tissue fibrosis in systemic sclerosis has also been verified by several groups of studies.[31] MCP1 is a chemokine that regulates the recruitment and activation of monocytes as well as promotes tissue fibrosis by stimulating the ECMs synthesis in SSc fibroblasts.[48] Our real-time qRT-PCR data demonstrated that the M2 macrophage marker *Cd206*, as well as *Mcp1/Ccl2*, were decreased on day 28 of bleomycin-treated skin in *Stat6*$^{-/-}$ mice as well as mice treated with AS1517499, suggesting that depletion/inhibition of STAT6 ameliorates the activation and recruitment of M2 macrophage. The activated M2 macrophages have been shown to release fibrotic cytokines including TGFβ1, IL-4, and IL-13.[49] Interestingly, our data also showed a decreased *Il13* level in *Stat6*$^{-/-}$ mice and mice treated with AS1517499, suggesting an association between M2 macrophage activation and IL-13 expression. Taken together, our findings indicated that STAT6 inhibition/depletion suppresses ECM production and skin fibrosis partially by suppressing the activation/recruitment of M2 macrophage and its subsequent release of fibrotic cytokines.

Although IL-4 and IL-13 shared common signaling pathways and both have demonstrated a role in tissue fibrosis, some studies suggested that IL-4 seems to play a dominant role in IgE synthesis in allergic diseases, and IL-13 acts predominantly in fibrosis.[20,50,51] It was demonstrated in the bleomycin-induced lung fibrosis model, that neutralizing IL-13 but not IL-4 decreased fibrosis in the lungs.[19] These findings are supported by the mice with transgenic overexpression of IL-13 in murine lungs showing enhanced pulmonary inflammation and fibrosis.[20,52] Similarly, only IL-13 but not IL-4 deficient mice showed reduced collagen synthesis and attenuated fibrosis in the fluorescein isothiocyanate-induced lung injury and fibrosis, and the IL-13 and IL-4 double knockout mice have no additive

protection compared to IL-13 knockout mice, suggesting that IL-13 plays a more essential role in this fibrosis model than IL-4.[53] Interestingly, in our study, we found that IL-13 but not IL-4 levels were decreased in the skin on day 28 *Stat6*$^{-/-}$ mice or AS1517499-injected mice in response to bleomycin. Our results are correlated with previous findings showing a major role of IL-13 in fibrosis and suggested that decreased IL-13 might partially account for declined skin fibrosis in *Stat6*$^{-/-}$ or AS1517499-treated mice. Further studies may be needed to understand the mechanism of reduced IL-13 released in response to injury in the *Stat6*$^{-/-}$ or AS1517499-treated skin, is it through M2 macrophage activation/recruitment?

In conclusion, our study demonstrated that STAT6 was activated in the fibrotic skin of patients with SSc and mice treated with bleomycin. We also confirmed in the bleomycin-induced murine model of skin fibrosis, that genetic *Stat6* depletion or pharmacological STAT6 inhibition prevented the expression of fibrogenic cytokines at the late fibrotic stages, reduced the production of ECMs, and attenuated skin fibrosis. In summary, our study suggested that STAT6 is a potent therapeutic target to control skin fibrosis in systemic sclerosis and other fibrotic diseases.

Supplementary Material

Refer to Web version on PubMed Central for supplementary material.

ACKNOWLEDGMENTS

This work was supported by NIH NIAMS 1R01AR073284 (SA & TM); R61AR078078 (SA); R56AR078211 (MW & SA); NIH NIA 1R56AG076144-01A1 (TM), Jiangsu Province Institute of Geriatrics Clinical Technology Application Research Project LD2022003 (JH), Leader of Jiangsu Province Geriatrics Clinical Technology Application Research Project LR2022 011 (JH), and the Healthy Aging Research Project of Jiangsu Provincial Health Commission LK2021030 (JH).

Funding information

National Institute of Arthritis and Musculoskeletal and Skin Diseases, Grant/Award Number: 1R01AR073284, R61AR078078 and R56AR078211; National Institute on Aging, Grant/Award Number: 1R56AG076144-01A1; The Healthy Aging Research Project of Jiangsu Provincial Health Commission, Grant/Award Number: LK2021030; Jiangsu Province Institute of Geriatrics Clinical Technology Application Research Project, Grant/Award Number: LD2022003; Leader of Jiangsu Province Geriatrics Clinical Technology Application Research Project, Grant/Award Number: LR2022 011

DATA AVAILABILITY STATEMENT

The data that support the findings of this study are available on request from the corresponding author.

Abbreviations:

CCL2	C-C motif chemokine ligand 2
COL1	type I collagen
CXCL1	chemokine (C-X-C motif) ligand 1
CXCL10	chemokine (C-X-C motif) ligand 10

CXCL2	chemokine (C-X-C motif) ligand 2
ECM	extracellular matrix
FN1	fibronectin
GENISOS	Genetic versus Environment In Scleroderma Outcome Study
IL13	interleukin 13
IL4	interleukin 4
Mac-3 (LAMP2)	lysosome-associated membrane protein 2
POSTN	periostin
SSc	systemic sclerosis
STAT6	Signal transducers and activators of transcription 6
TGFβ	Transforming growth factor-β
TSK1	tight skin 1

REFERENCES

1. Allanore Y, Simms R, Distler O, et al. Systemic sclerosis. Nat Rev Dis Primers. 2015;1:15002. [PubMed: 27189141]
2. Ho YY, Lagares D, Tager AM, Kapoor M. Fibrosis–a lethal component of systemic sclerosis. Nat Rev Rheumatol. 2014;10:390–402. [PubMed: 24752182]
3. Lafyatis R Transforming growth factor beta–at the Centre of systemic sclerosis. Nat Rev Rheumatol. 2014;10:706–719. [PubMed: 25136781]
4. Hasegawa M, Fujimoto M, Kikuchi K, Takehara K. Elevated serum levels of interleukin 4 (IL-4), IL-10, and IL-13 in patients with systemic sclerosis. J Rheumatol. 1997;24:328–332. [PubMed: 9034992]
5. Jinnin M, Ihn H, Yamane K, Tamaki K. Interleukin-13 stimulates the transcription of the human alpha2(I) collagen gene in human dermal fibroblasts. J Biol Chem. 2004;279:41783–41791. [PubMed: 15271999]
6. Bhogal RK, Bona CA. Regulatory effect of extracellular signal-regulated kinases (ERK) on type I collagen synthesis in human dermal fibroblasts stimulated by IL-4 and IL-13. Int Rev Immunol. 2008;27:472–496. [PubMed: 19065352]
7. Wen FQ, Kohyama T, Liu X, et al. Interleukin-4- and interleukin-13-enhanced transforming growth factor-beta2 production in cultured human bronchial epithelial cells is attenuated by interferon-gamma. Am J Respir Cell Mol Biol. 2002;26:484–490. [PubMed: 11919085]
8. Lee CG, Homer RJ, Zhu Z, et al. Interleukin-13 induces tissue fibrosis by selectively stimulating and activating transforming growth factor beta(1). J Exp Med. 2001;194:809–821. [PubMed: 11560996]
9. McGaha T, Saito S, Phelps RG, et al. Lack of skin fibrosis in tight skin (TSK) mice with targeted mutation in the interleukin-4R alpha and transforming growth factor-beta genes. J Invest Dermatol. 2001;116:136–143. [PubMed: 11168809]
10. McCormick SM, Heller NM. Commentary: IL-4 and IL-13 receptors and signaling. Cytokine. 2015;75:38–50. [PubMed: 26187331]
11. McGaha TL, Bona CA. Role of profibrogenic cytokines secreted by T cells in fibrotic processes in scleroderma. Autoimmun Rev. 2002;1:174–181. [PubMed: 12849012]

12. Patel BK, Wang LM, Lee CC, Taylor WG, Pierce JH, LaRochelle WJ. Stat6 and Jak1 are common elements in platelet-derived growth factor and interleukin-4 signal transduction pathways in NIH 3T3 fibroblasts. J Biol Chem. 1996;271:22175–22182. [PubMed: 8703030]
13. Goenka S, Kaplan MH. Transcriptional regulation by STAT6. Immunol Res. 2011;50:87–96. [PubMed: 21442426]
14. Murata T, Husain SR, Mohri H, Puri RK. Two different IL-13 receptor chains are expressed in normal human skin fibroblasts, and IL-4 and IL-13 mediate signal transduction through a common pathway. Int Immunol. 1998;10:1103–1110. [PubMed: 9723696]
15. Wynn TA. Fibrotic disease and the T_H1/T_H2 paradigm. Nat Rev Immunol. 2004;4:583–594. [PubMed: 15286725]
16. Huang XL, Wang YJ, Yan JW, et al. Role of anti-inflammatory cytokines IL-4 and IL-13 in systemic sclerosis. Inflamm Res. 2015;64:151–159. [PubMed: 25725697]
17. Mueller R, Krahl T, Sarvetnick N. Pancreatic expression of interleukin-4 abrogates insulitis and autoimmune diabetes in nonobese diabetic (NOD) mice. J Exp Med. 1996;184:1093–1099. [PubMed: 9064326]
18. Ong C, Wong C, Roberts CR, Teh HS, Jirik FR. Anti-IL-4 treatment prevents dermal collagen deposition in the tight-skin mouse model of scleroderma. Eur J Immunol. 1998;28:2619–2629. [PubMed: 9754550]
19. Belperio JA, Dy M, Burdick MD, et al. Interaction of IL-13 and C10 in the pathogenesis of bleomycin-induced pulmonary fibrosis. Am J Respir Cell Mol Biol. 2002;27:419–427. [PubMed: 12356575]
20. O'Reilly S Role of interleukin-13 in fibrosis, particularly systemic sclerosis. Biofactors. 2013;39:593–596. [PubMed: 23893513]
21. Allanore Y, Wung P, Soubrane C, et al. A randomised, double-blind, placebo-controlled, 24-week, phase II, proof-of-concept study of romilkimab (SAR156597) in early diffuse cutaneous systemic sclerosis. Ann Rheum Dis. 2020;79:1600–1607. [PubMed: 32963047]
22. Morin F, Kavian N, Chouzenoux S, et al. Leflunomide prevents ROS-induced systemic fibrosis in mice. Free Radic Biol Med. 2017;108:192–203. [PubMed: 28365359]
23. Cheng E, Zhang X, Wilson KS, et al. JAK-STAT6 pathway inhibitors block Eotaxin-3 secretion by epithelial cells and fibroblasts from esophageal eosinophilia patients: promising agents to improve inflammation and prevent fibrosis in EoE. PLoS One. 2016;11:e0157376. [PubMed: 27310888]
24. Yamamoto T, Takagawa S, Katayama I, et al. Animal model of sclerotic skin. I: local injections of bleomycin induce sclerotic skin mimicking scleroderma. J Invest Dermatol. 1999;112:456–462. [PubMed: 10201529]
25. Yamamoto T, Nishioka K. Cellular and molecular mechanisms of bleomycin-induced murine scleroderma: current update and future perspective. Exp Dermatol. 2005;14:81–95. [PubMed: 15679577]
26. Kaplan MH, Schindler U, Smiley ST, Grusby MJ. Stat6 is required for mediating responses to IL-4 and for development of Th2 cells. Immunity. 1996;4:313–319. [PubMed: 8624821]
27. Peoples C, Medsger TA Jr, Lucas M, Rosario BL, Feghali-Bostwick CA. Gender differences in systemic sclerosis: relationship to clinical features, serologic status and outcomes. J Scleroderma Relat Disord. 2016;1:177–240.
28. Takagawa S, Lakos G, Mori Y, Yamamoto T, Nishioka K, Varga J. Sustained activation of fibroblast transforming growth factor-beta/Smad signaling in a murine model of scleroderma. J Invest Dermatol. 2003;121:41–50. [PubMed: 12839562]
29. O'Reilly S, Ciechomska M, Fullard N, Przyborski S, van Laar JM. IL-13 mediates collagen deposition via STAT6 and microRNA-135b: a role for epigenetics. Sci Rep. 2016;6:25066. [PubMed: 27113293]
30. Wynn TA, Vannella KM. Macrophages in tissue repair, regeneration, and fibrosis. Immunity. 2016;44:450–462. [PubMed: 26982353]
31. Stifano G, Christmann RB. Macrophage involvement in systemic sclerosis: do we need more evidence? Curr Rheumatol Rep. 2016;18:2. [PubMed: 26700912]
32. Ding J, Tredget EE. The role of chemokines in fibrotic wound healing. Adv Wound Care (New Rochelle). 2015;4:673–686. [PubMed: 26543681]

33. Juhas U, Ryba-Stanislawowska M, Szargiej P, Mysliwska J. Different pathways of macrophage activation and polarization. Postepy Hig Med Dosw (Online). 2015;69:496–502. [PubMed: 25983288]
34. Jiao B, An C, Tran M, et al. Pharmacological inhibition of STAT6 ameliorates myeloid fibroblast activation and alternative macrophage polarization in renal fibrosis. Front Immunol. 2021;12:735014. [PubMed: 34512669]
35. Mitamura Y, Nunomura S, Nanri Y, et al. Hierarchical control of interleukin 13 (IL-13) signals in lung fibroblasts by STAT6 and SOX11. J Biol Chem. 2018;293:14646–14658. [PubMed: 30076218]
36. Zhao J, Okamoto Y, Asano Y, et al. Sphingosine-1-phosphate receptor-2 facilitates pulmonary fibrosis through potentiating IL-13 pathway in macrophages. PLoS One. 2018;13:e0197604. [PubMed: 29782549]
37. Nikota J, Banville A, Goodwin LR, et al. Stat-6 signaling pathway and not Interleukin-1 mediates multi-walled carbon nanotube-induced lung fibrosis in mice: insights from an adverse outcome pathway framework. Part Fibre Toxicol. 2017;14:37. [PubMed: 28903780]
38. Yan J, Zhang Z, Yang J, Mitch WE, Wang Y. JAK3/STAT6 stimulates bone marrow-derived fibroblast activation in renal fibrosis. J Am Soc Nephrol. 2015;26:3060–3071. [PubMed: 26032813]
39. Ong CJ, Ip S, Teh SJ, et al. A role for T helper 2 cells in mediating skin fibrosis in tight-skin mice. Cell Immunol. 1999;196:60–68. [PubMed: 10486156]
40. Homann D, Holz A, Bot A, et al. Autoreactive CD4+ T cells protect from autoimmune diabetes via bystander suppression using the IL-4/Stat6 pathway. Immunity. 1999;11:463–472. [PubMed: 10549628]
41. Chitnis T, Najafian N, Benou C, et al. Effect of targeted disruption of STAT4 and STAT6 on the induction of experimental autoimmune encephalomyelitis. J Clin Invest. 2001;108:739–747. [PubMed: 11544280]
42. Antonelli A, Ferri C, Fallahi P, et al. CXCL10 (alpha) and CCL2 (beta) chemokines in systemic sclerosis–a longitudinal study. Rheumatology (Oxford). 2008;47:45–49. [PubMed: 18077490]
43. Crescioli C, Corinaldesi C, Riccieri V, et al. Association of circulating CXCL10 and CXCL11 with systemic sclerosis. Ann Rheum Dis. 2018;77:1845–1846. [PubMed: 29760155]
44. Fabre T, Molina MF, Soucy G, et al. Type 3 cytokines IL-17A and IL-22 drive TGF-beta-dependent liver fibrosis. Sci Immunol. 2018;3:eaar7754. [PubMed: 30366940]
45. Zhang HJ, Zhang YN, Zhou H, Guan L, Li Y, Sun MJ. IL-17A promotes initiation and development of intestinal fibrosis through EMT. Dig Dis Sci. 2018;63:2898–2909. [PubMed: 30097894]
46. Puccetti M, Paolicelli G, Oikonomou V, et al. Towards targeting the aryl hydrocarbon receptor in cystic fibrosis. Mediators Inflamm. 2018;2018:1601486. [PubMed: 29670460]
47. Chizzolini C, Dufour AM, Brembilla NC. Is there a role for IL-17 in the pathogenesis of systemic sclerosis? Immunol Lett. 2018;195:61–67. [PubMed: 28919455]
48. Distler JH, Akhmetshina A, Schett G, Distler O. Monocyte chemoattractant proteins in the pathogenesis of systemic sclerosis. Rheumatology (Oxford). 2009;48:98–103. [PubMed: 18984611]
49. Raker V, Haub J, Stojanovic A, Cerwenka A, Schuppan D, Steinbrink K. Early inflammatory players in cutanous fibrosis. J Dermatol Sci. 2017;87:228–235. [PubMed: 28655471]
50. Parulekar AD, Diamant Z, Hanania NA. Role of T2 inflammation biomarkers in severe asthma. Curr Opin Pulm Med. 2016;22:59–68. [PubMed: 26574724]
51. Passalacqua G, Mincarini M, Colombo D, et al. IL-13 and idiopathic pulmonary fibrosis: possible links and new therapeutic strategies. Pulm Pharmacol Ther. 2017;45:95–100. [PubMed: 28501346]
52. Zhu Z, Homer RJ, Wang Z, et al. Pulmonary expression of interleukin-13 causes inflammation, mucus hypersecretion, subepithelial fibrosis, physiologic abnormalities, and eotaxin production. J Clin Invest. 1999;103:779–788. [PubMed: 10079098]
53. Kolodsick JE, Toews GB, Jakubzick C, et al. Protection from fluorescein isothiocyanate-induced fibrosis in IL-13-deficient, but not IL-4-deficient, mice results from impaired collagen synthesis by fibroblasts. J Immunol. 2004;172:4068–4076. [PubMed: 15034018]

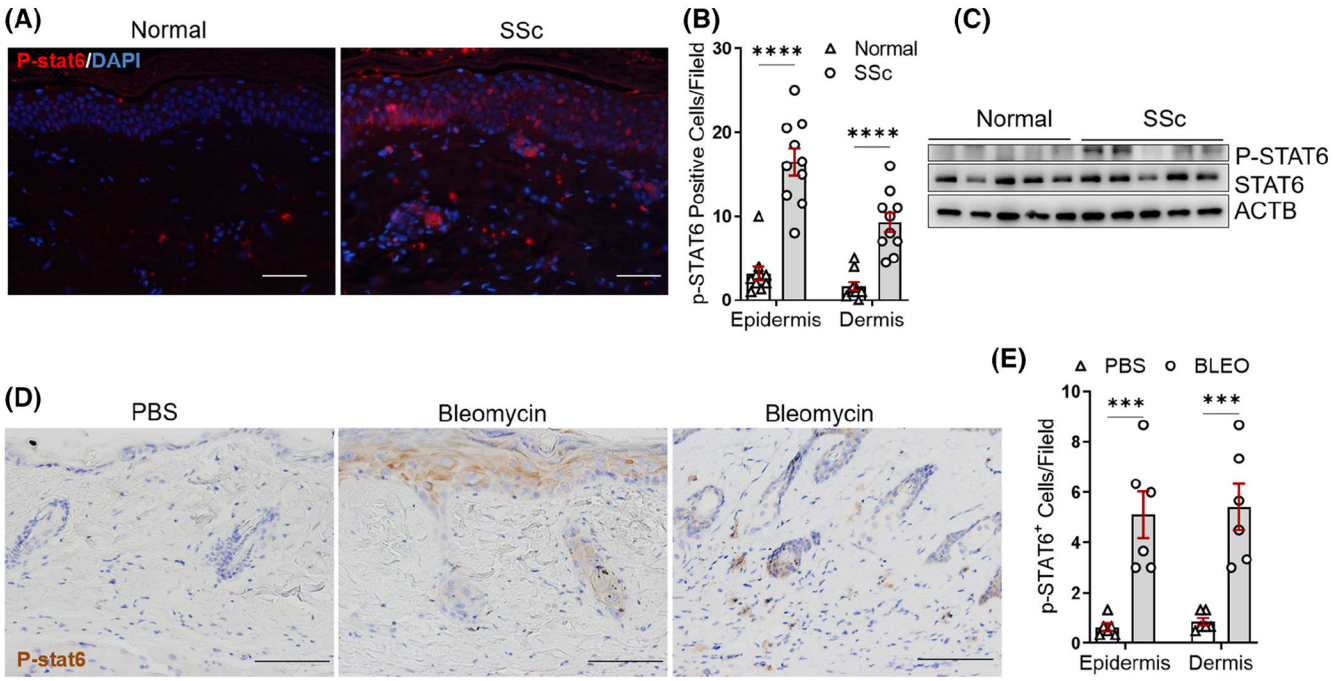

FIGURE 1.

STAT6 phosphorylation is increased in SSc skin. (A) Human healthy and SSc skin tissues were stained using p-STAT6 (red) antibodies. DAPI was used to stain the nucleus (blue). Scale bar = 200 μm. Representative images. n = 10/group. (B) The number of p-STAT6-positive cells at the epidermal and dermal layer per high power field was blindly counted in 10 normal and 10 SSc skin. (C) The protein levels of p-STAT6 and STAT6 were determined by western blot in the primary skin fibroblasts isolated from healthy donors or SSc patients. (D) Immunohistochemistry (IHC) was performed to stain p-STAT6 in day 28 PBS or bleomycin-injected murine skin. N = 6/group. Scale bar = 200 μm. (E) The number of p-STAT6-positive cells was blindly counted in six control and six bleomycin-injected mouse lesional skin. Data were presented as means ± mean squared error (MSE). p-value was calculated using ANOVA followed by Sidak-adjusted multiple comparisons. ***$p < .001$, ****$p < .0001$

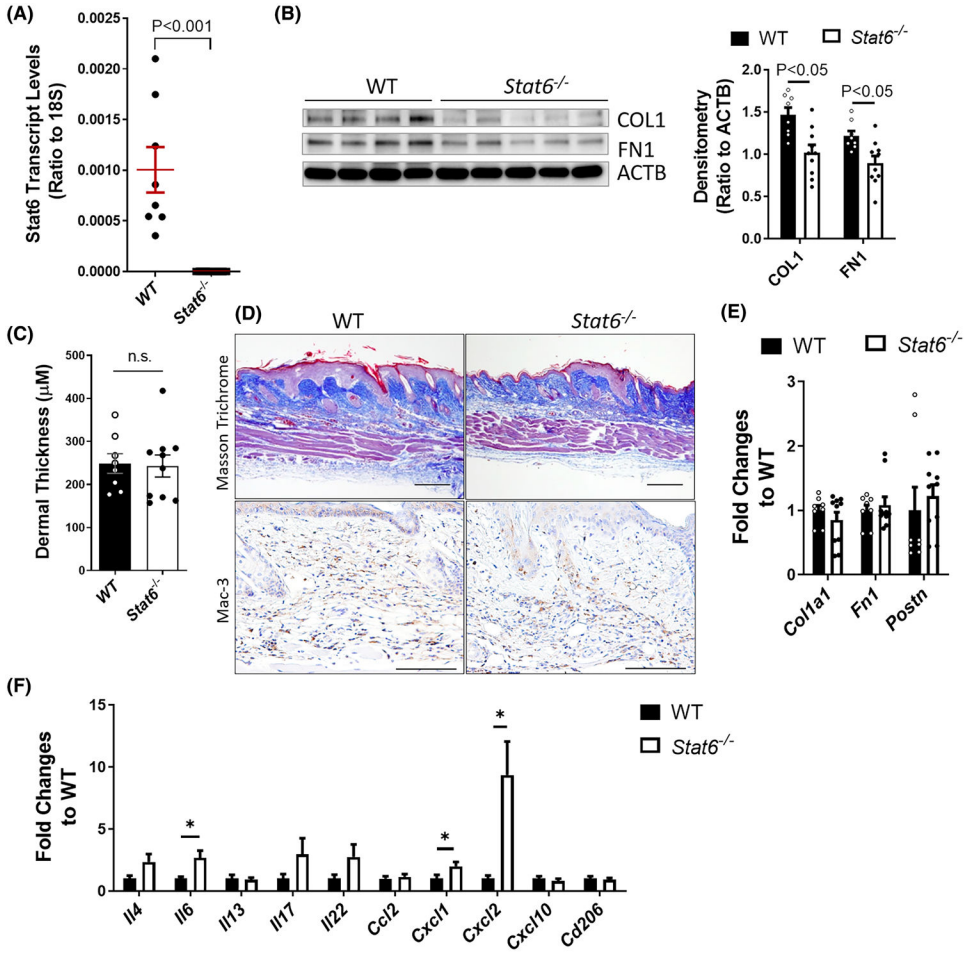

FIGURE 2.

STAT6 depletion had limited effect on bleomycin-induced skin fibrosis on day 14. Wildtype (WT) or *Stat6* knockout (*Stat6*$^{-/-}$) mice were subcutaneously injected with bleomycin (0.02 U/mouse/day) six times a week for 2 weeks. (A) The transcript levels of *Stat6* in the skin of WT and *Stat6*$^{-/-}$ mice. Data are presented as a ratio to 18 S rRNA. (B) Left panel: Skin was collected on day 14 for western blot analysis to determine the expression of fibrotic marker collagen I (COL1) and fibronectin (FN1). β-Actin (ACTB) was used as an internal control. Right panel: The densitometry of the western blot image was measured and data were presented as (ratio to actin) ± MSE. (C) The skin thickness was measured blindly for each group. The graph represents means ± standard error. (D) Masson's trichrome staining was carried out to determine the collagen deposition and IHC for Mac-3 was performed to determine the number of macrophages. Representative images for each group (n = 10 per group) are shown. Scale bar= 250 μm. (E and F) The transcript expression of (E) fibrotic markers *Col1a1, Fn1*, and *Postn*, and (F) cytokines *Il4, Il13, Il6, Il17, Il22, Ccl2, Cxcl1, Cxcl2, Cxcl10*, and *Cd206* were determined using real-time qRT-PCR in the skin of day 14 bleomycin-injected WT or *Stat6*$^{-/-}$ mice. The transcript expression of β-actin (*Actb*) was also determined and used as a reference. The graph represents the mean ratio to WT control ± MSE. p value was calculated using a two-tailed Student's t-test. *$p < .05$

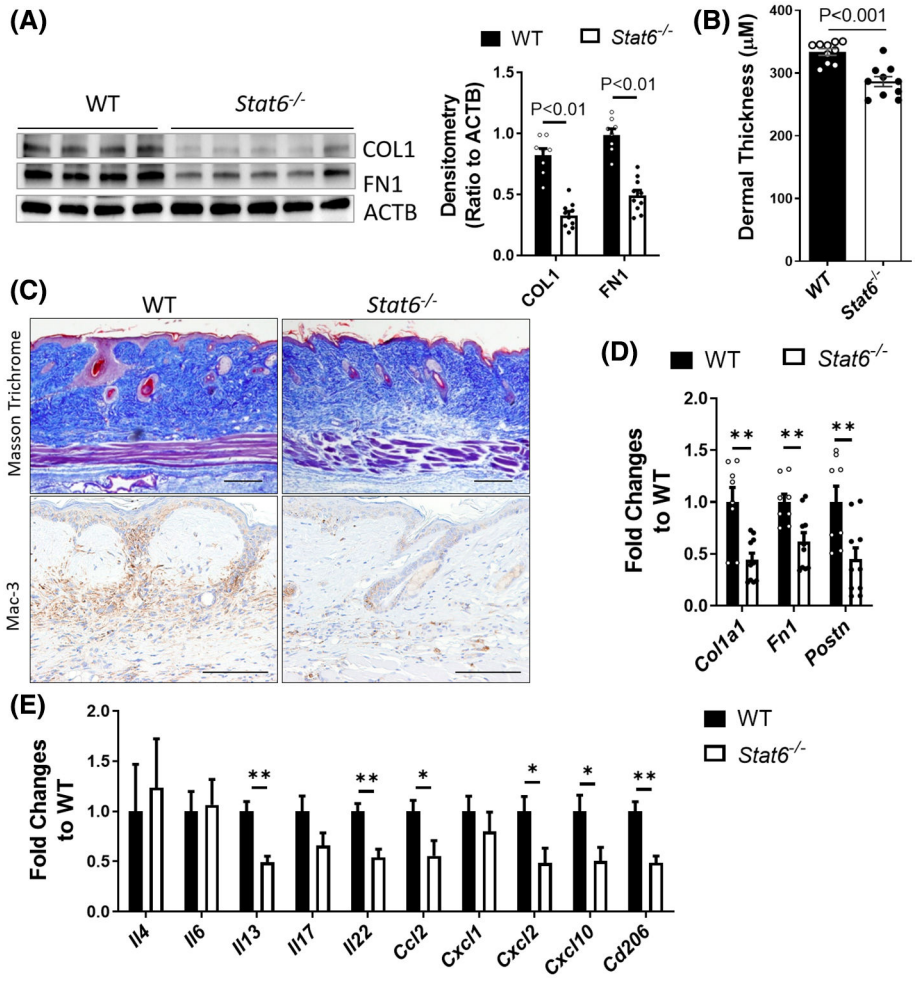

FIGURE 3.

Bleomycin-induced skin fibrosis was attenuated in *Stat6*$^{-/-}$ mice on day 28. Wildtype (WT) or *Stat6* knockout (*Stat6*$^{-/-}$) mice were subcutaneously injected with bleomycin (0.02 U/mouse/day) six times a week for 4 weeks. The skin was collected on day 28 for analysis. (A) Left panel: Western blot was used to determine the expression of fibrotic marker COL1 and FN1. Actin was used as an internal control. Right panel: The densitometry of the COL1 and FN1 was analyzed and data were presented as (ratio to ACTB) ± MSE. (B) The skin thickness was measured using Masson's trichrome stained images ($n = 10$). The graph represents means ± MSE. (C) Masson's trichrome staining and IHC for Mac-3 were performed to determine the collagen deposition and the number of macrophages, respectively. Scale bar= 250 μm. The transcript expression of (D) fibrotic markers *Col1a1, Fn1*, and *Postn*, and (E) cytokines *Il4, Il13, Il6, Il17, Il22, Ccl2, Cxcl1, Cxcl2, Cxcl10*, and *Cd206* were determined using real-time qRT-PCR in the skin of day 28 bleomycin-injected WT or *Stat6*$^{-/-}$ mice. Data were first normalized to the transcript levels of *Actb*, and then calculated as a ratio to WT control. The graph represents means ± MSE. *p* value was calculated using two-tailed Student's *t*-tests. *$p < .05$, **$p < .01$

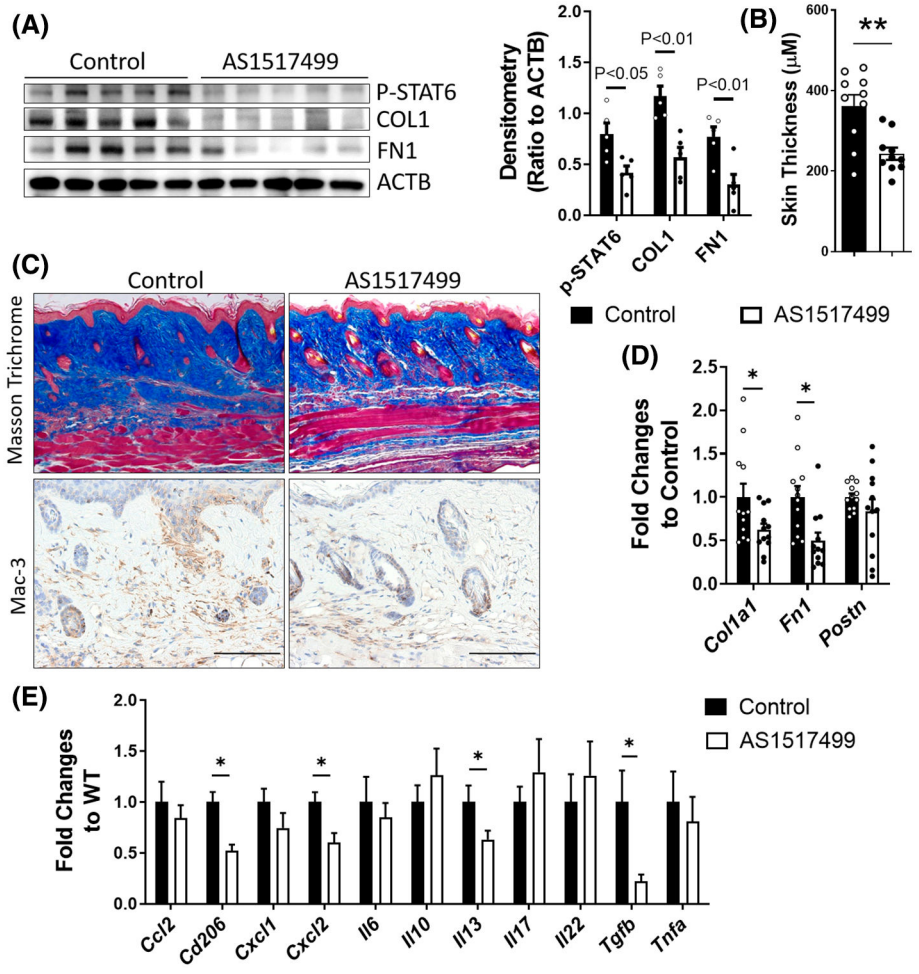

FIGURE 4.

AS1517499 attenuates bleomycin-induced skin fibrosis. WT mice were subcutaneously injected with bleomycin (0.02 U/mouse/day) six times a week for 4 weeks. Starting 1 week after the first bleomycin injection, mice were subcutaneously injected with 100 μl 20% DMSO or AS1517499 (0.5 mg/ml in 20% DMSO) twice a week at the same bleomycin injection sites. The skin was collected on day 28 for analysis. (A) Left panel: Western blot was used to determine the expression of p-STAT6, fibrotic markers COL1, and FN1. ACTB was used as an internal control. Right panel: The densitometry of the COL1 and FN1 was analyzed and data were presented as (ratio to ACTB) ± MSE. $N = 5$. (B) The skin thickness was measured using Masson's trichrome stained images ($n = 10$). The graph represents means ± MSE. (C) Masson's trichrome staining was performed to determine the collagen deposition and IHC for Mac-3 was performed to determine the number of macrophages. Scale bar= 250 μm. The transcript expression of (D) fibrotic markers *Col1a1, Fn1*, and *Postn*, and (E) cytokines *Ccl2, Cd206, Cxcl1, Cxcl2, Il6, Il10, Il13, Il17, Il22, Tgfb*, and tumor necrosis factor alpha (*Tnfa*) were determined using real-time qRT-PCR. Data were first normalized to the transcript levels of *Actb* and then calculated as a ratio to WT control. The graph represents means ± MSE. p value was calculated using two-tailed Student's t-tests. *$p < .05$, **$p < .01$

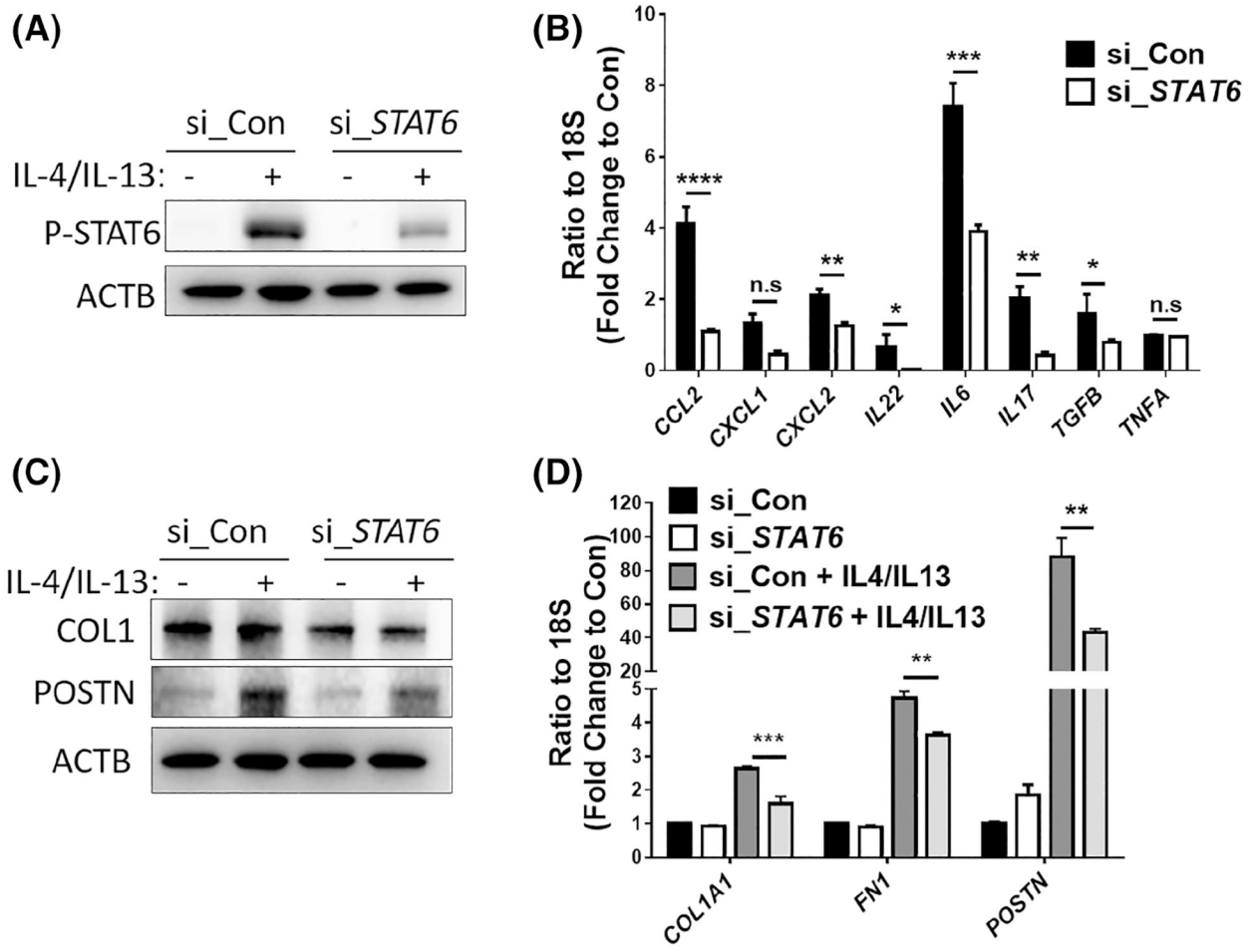

FIGURE 5.

The keratinocyte STAT6 promotes fibrotic marker expression in co-cultured fibroblasts. STAT6 was knocked down in skin keratinocyte HaCaT cells using siRNA (50 picomole/ml). Two days after transfection, cells were stimulated with IL-4/IL-13 (10 ng/ml each). (A) Western blot analysis demonstrated the protein levels of phosphorylated STAT6 2 h after IL-4/13 treatment. β-Actin was used as the internal control. (B) The transcript levels of *CCL2, CXCL1, CXCL2, IL22, IL6, IL17, TGFB1*, and *TNFA were* determined using real-time qRT-PCR in the keratinocytes treated with IL-4/13 for 6 h. Data were shown as fold change to control siRNA transfected cells without IL-4/IL-13 treatment ± MSE. (C and D) HaCaT cells were transfected with control or STAT6 siRNA and 2 days later treated with IL-4/IL-13 for 6 h. The medium for HaCaT cells was then changed to IL-4/IL-13 free media, and the keratinocytes were co-cultured with primary skin fibroblasts in inserts for additional 24 h. (C) Western blot analysis shows fibrotic marker expression in co-cultured skin fibroblasts. (D) Real-time qRT-PCR was performed to examine the levels of fibrotic markers in co-cultured skin fibroblasts. Data are shown as fold change to control fibroblasts co-cultured with control siRNA-treated keratinocyte ± MSE. Two-tailed Student's *t*-test was used for data analysis, data were corrected for multiple comparisons using a false discovery rate. *FDR <0.05, **FDR <0.01, ***FDR <0.001, ****FDR <0.0001

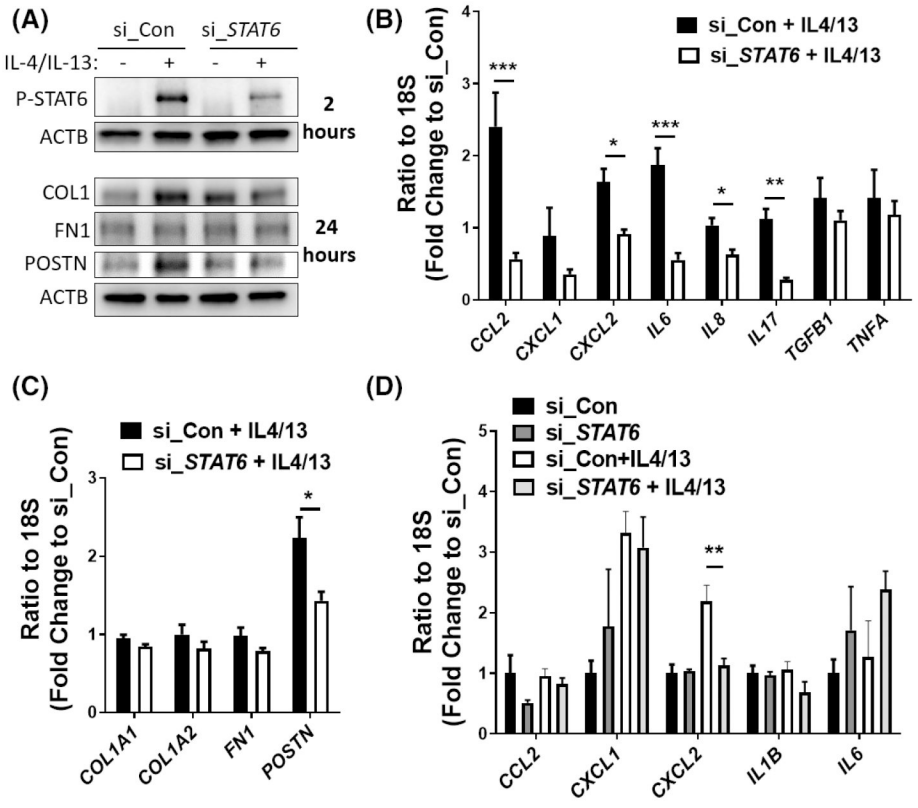

FIGURE 6.

Fibroblast STAT6 promotes CXCL2 expression in co-cultured Keratinocytes. Primary skin fibroblasts were transfected with control (si_Con) or STAT6 siRNA (si_*STAT6*) (50 picomole/ml). Two days after transfection, cells were stimulated with IL-4/IL-13 (10 ng/ml each) for 6 h. (A) Western blot analysis demonstrated the protein levels of phosphorylated STAT6 2 h after IL-4/−13 treatment, and levels of COL1, FN1 and POSTN 24 h after IL-4/−13 treatment. β-Actin was used as the internal control. (B and C) The transcript levels of (B) cytokines (*CCL2, CXCL1, CXCL2, IL6, IL8, IL17, TGFB1*, and *TNFA*) and (C) fibrotic markers (*COL1A1, COL1A2, FN1*, and *POSTN*) were determined using real-time qRT-PCR in fibroblasts. Data were shown as fold change to control siRNA transfected cells without IL-4/IL-13 treatment ± MSE. (D) Fibroblasts with *STAT6* knockdown were treated with IL-4/IL-13 for 6 h. Then the fibroblast medium was changed to IL-4/IL-13 free media, and the fibroblasts were co-cultured with HaCaT (in an insert) for additional 24 h. Real-time qRT-PCR was performed to examine the levels of cytokines in co-cultured HaCaT. Data are shown as fold change to si_Con ± MSE. Two-tailed Student's *t*-test was used for data analysis, data were corrected for multiple comparisons using a false discovery rate. *FDR <0.05, **FDR <0.01, ***FDR <0.001